



# Boride-induced dislocation channeling in a single crystal Ni-based superalloy

H.L. Ge<sup>a,b</sup>, J.D. Liu<sup>c</sup>, S.J. Zheng<sup>a,\*</sup>, Y.T. Zhou<sup>a</sup>, Q.Q. Jin<sup>a</sup>, X.H. Shao<sup>a</sup>, B. Zhang<sup>a</sup>, Y.Z. Zhou<sup>c,\*</sup>, X.L. Ma<sup>a,d</sup>

<sup>a</sup>Shenyang National Laboratory for Materials Science, Institute of Metal Research, Chinese Academy of Sciences, 110016 Shenyang, China

<sup>b</sup>School of Materials Science and Engineering, University of Science and Technology of China, 230026 Hefei, China

<sup>c</sup>Superalloys Division, Institute of Metal Research, Chinese Academy of Sciences, 110016 Shenyang, China

<sup>d</sup>School of Material Science and Engineering, Lanzhou University of Technology, 730050 Lanzhou, China



## ARTICLE INFO

### Article history:

Received 19 July 2018

Received in revised form 28 September 2018

Accepted 6 October 2018

Available online 8 October 2018

### Keywords:

Ni-based superalloy

Creep

Boride

Dislocation

Interface

## ABSTRACT

Generally, minor elements such as carbon and boron are added in superalloys to strengthen grain boundaries. However, effects of carbon and boron on single crystal superalloys remain disputed. Here we demonstrate that  $M_{23}B_6$  (where M is mixture of W, Mo, Cr and Ni) can induce dislocation channeling in a Ni-based single crystal superalloy. The  $M_{23}B_6$  has a cube-on-cube orientation relationship with the matrix, forming a majority of {1 1 1} plane interfaces. Furthermore, the atomic stepped {1 1 1} interface could facilitate dislocation nucleation. Dislocations emitted from the interface glide forward and pile-up in the channel, resulting in strain localization and creep micro-crack initiation.

© 2018 Published by Elsevier B.V.

## 1. Introduction

Grain boundary strengthening elements such as carbon and boron were initially eliminated from single crystal superalloys. Additions of these elements are considered particularly to lower incipient melting temperatures in single crystal superalloys [1,2]. However, owing to high complexity of hollow structure of blades, low-angle grain boundaries (LAGBs) are almostly unavoidable. Recently, minor additions of C and B have been shown to strengthen LAGBs that may form during single crystal casting, and can also effectively increase allowable LAGB misorientation angles [3–6].

Owing to the low solubility of B in superalloys, presence of boride is inevitable in single crystal superalloys [7]. Boride precipitates definitely affect the creep deformation behavior. In the tertiary creep regime, damage develops in the form of cavity nucleating and growing from casting porosity and secondary phases, such as TCP phases, carbides and borides in single crystal superalloys [8]. However, in carbon containing nickel-based single crystal superalloys, it was supposed that a small amount of MC and nano-sized  $M_{23}C_6$  carbides could block the dislocation movement and enhance the creep properties [9]. Consequently, the effect of carbides/

borides on the creep behaviors is related to the corresponding dislocation behaviors. Many investigations have focused on the dislocation behaviors in the matrix ( $\gamma/\gamma'$ ) under high-temperature and low-stress creep in single crystal superalloys [10–13], but solid experimental investigations of dislocation behaviors related to carbides/borides have not been reported.

This work aims to investigate the details of dislocation activity associated with the interface between borides and matrix using transmission electron microscopy (TEM). In the traditional view, creep crack initiation is generally associated with interface debonding at second-phase particles. Here, the results suggest that borides at  $\gamma'$  interior could act as a source of dislocation channel. The formation mechanism of boride-induced dislocation channeling is proposed.

## 2. Materials and methods

Focusing on the boride effect on the creep deformation, the crept microstructure of a single crystal superalloy joint bonded with boron containing interlayer through transient liquid phase (TLP) bonding were investigated in the present work. The nominal composition (wt%) of the base alloy is 6.0Cr, 7.5Co, 1.2Mo, 5.8 W, 5.9Al, 1.1Ti, and balance by Ni. And the interlayer composition is 15Cr, 3.5B, and balance by Ni. After TLP bonding and heat treatment [14], the specimens were machined into stress rupture

\* Corresponding authors.

E-mail addresses: [sjzheng@imr.ac.cn](mailto:sjzheng@imr.ac.cn) (S.J. Zheng), [yzzhou@imr.ac.cn](mailto:yzzhou@imr.ac.cn) (Y.Z. Zhou).

samples with a gauge diameter of 5 mm and a gauge length of 25 mm. Stress rupture samples were tested at 982 °C/248 MPa.

TEM samples were taken from the joint adjacent to the fracture surface. The microstructural observation and composition analysis were conducted on a Titan Cube 60–300, equipped with a high angle annular dark field (HAADF) detector, energy-dispersive X-ray (EDX) detector and Gatan Quantum energy loss (EELS) spectrometer. Selected area electron diffraction (SAED) patterns were recorded in a JEOL 2100 microscope.

### 3. Results and discussion

An overview of the crept microstructure is illustrated in an HAADF image of Fig. 1a. The sample presents typical features of creep, such as  $\gamma'$  coarsening. Interestingly, as marked with a black square at the bottom-left of Fig. 1a, a precipitate enriched with heavy elements and heading a deformation band can be seen in the matrix. And a crack formed ahead of the deformation band away from the precipitate. In Fig. 1b, a higher magnified image indicates that the deformation band is a dislocation channel. Moreover, it seems that the dislocations come from the interface between the precipitate and the matrix. Furthermore, as the results showing, the dislocations in the channel could slip through  $\gamma$  and  $\gamma'$  directly. Dislocation pile-up in the channel could result in high local strain and an increase susceptibility of crack initiation which strongly influences creep performance. So in the following sections, we will identify the precipitate, characterize the interface feature between the precipitate and matrix, demonstrate Burgers vector of the dislocations, and propose the formation mechanism of the dislocation channeling.

The crystal structure and interface structure of the precipitate are identified as shown in Fig. 2. As shown in Fig. 2a, the precipitate with a size about 500 nm shown a polygonal shape. SAED patterns (Fig. 2b and c) indicate that the precipitate possibly corresponds to  $M_{23}C_6$  or  $M_{23}B_6$ . According to the EDS spectrum (Fig. 2d) acquired from the precipitate, the precipitate is mainly composed of W, Mo, Cr, Ni and a small amount of Co.  $M_{23}C_6$  carbide is based on  $Cr_{23}C_6$  while  $M_{23}B_6$  boride has a relatively high content of Ni [15,16]. In addition to the precipitate does not contain C, and the B signal was found in the EELS profile (inset in Fig. 2d), the precipitate can be determined as  $M_{23}B_6$ . And the orientation relationship (OR) can be determined as  $[1\ 0\ 0]_M // [1\ 0\ 0]_B$  and  $[1\ 1\ 0]_M // [1\ 1\ 0]_B$  (in Fig. 2b and c), where subscript M and B represent matrix and boride, respectively. As the superlattice reflections  $\{0\ 0\ 1\}$  and

$\{0\ 1\ 1\}$  of  $\gamma'$  can be seen in the SAED patterns, it's safe to deduced that  $M_{23}B_6$  is in the  $\gamma'$  phase. Based on the presented SAED patterns, the lattice constant of  $M_{23}B_6$  is 1.088 nm, which is approximately triple that of the  $\gamma'$  ( $a = 0.359$  nm). According to the high resolution HAADF images in Fig. 2e and f, the interfaces between  $M_{23}B_6$  and  $\gamma'$  are composed of low-index planes such as  $\{1\ 1\ 1\}_{\gamma' / M_{23}B_6}$  and  $\{0\ 0\ 1\}_{\gamma' / M_{23}B_6}$ , and the  $\{1\ 1\ 1\}_{\gamma' / M_{23}B_6}$  makes up the majority. The interface energy between  $M_{23}B_6$  and  $\gamma'$  can be greatly reduced by combination with low-index planes.

The dislocation configurations in the dislocation channel are clarified by two-beam diffraction contrast in Fig. 3. Fig. 3a–c show images of channeling dislocations using  $g\bar{1}\bar{1}1$ ,  $g0\bar{2}0$  and  $g0\bar{2}2$  reflections, respectively. We note that the dislocations labeled with I (in Fig. 3a) are visible for  $g\bar{1}\bar{1}1$  and almost out of contrast for  $g0\bar{2}0$  and  $g0\bar{2}2$  reflection. In addition, a small quantity of dislocations labeled with II (in Fig. 3b) are out of contrast for  $g\bar{1}\bar{1}1$  and  $g0\bar{2}2$ , and in contrast for  $g0\bar{2}0$ . Based on  $\mathbf{g} \cdot \mathbf{b} = 0$  invisibility criterion, these observations indicate that the I type dislocations have Burgers vector of  $a[1\ 0\ 0]$ , where  $a$  is the lattice constant, and II type dislocations have Burgers vector of  $a/2[0\ 1\ 1]$ . The TEM observations also show that the  $\gamma'$  regions except dislocation channel remain nearly free of dislocations though in the very late stage of the creep deformation. And previous studies have shown that a  $a[1\ 0\ 0]$  dislocation in  $\gamma'$  always has two different  $a/2[1\ 1\ 0]$  dislocation segments at the  $\gamma/\gamma'$  interface [10–13]. This implies that the channeling dislocations unlikely come from  $\gamma$  channels. More evidently, as shown in Fig. 3d, a single dislocation lies on a  $M_{23}B_6$ - $\gamma'$  interface, which indicates that these  $a[1\ 0\ 0]$  dislocations were possibly emitted from the  $\{1\ 1\ 1\}_{M_{23}B_6} // \{1\ 1\ 1\}_{\gamma'}$  interface.

Interfaces usually impede dislocation motion due to the crystallographic mismatch across an interface and the atomic disorder in an interface [17]. On the contrary, the phenomenon of interfaces acting as a source of dislocations has been revealed here. Dislocation nucleation is correlated to interface structure. As shown in Fig. 3e, stepped  $(1\ \bar{1}\ 1)_{\gamma'} // (1\ \bar{1}\ 1)_{M_{23}B_6}$  interface can be seen from  $[1\ 1\ 0]_{M_{23}B_6} // [1\ 1\ 0]_{\gamma'}$  direction. Each step is as high as three  $\gamma'$   $(1\ \bar{1}\ 1)$  atomic interplanes, which is consistent with that the lattice constant of  $M_{23}B_6$  is about triple that of  $\gamma'$ . In contrast to dislocation nucleation from atomically flat low energy interfaces, a much lower activation energy is required to nucleate dislocations from stepped or faceted interfaces [18,19]. During tension loading along  $[0\ 0\ 1]$  direction, the stepped  $\{1\ 1\ 1\}$  plane interfaces have higher resistance to interface shearing, consequently facilitate the emission of dislocations.

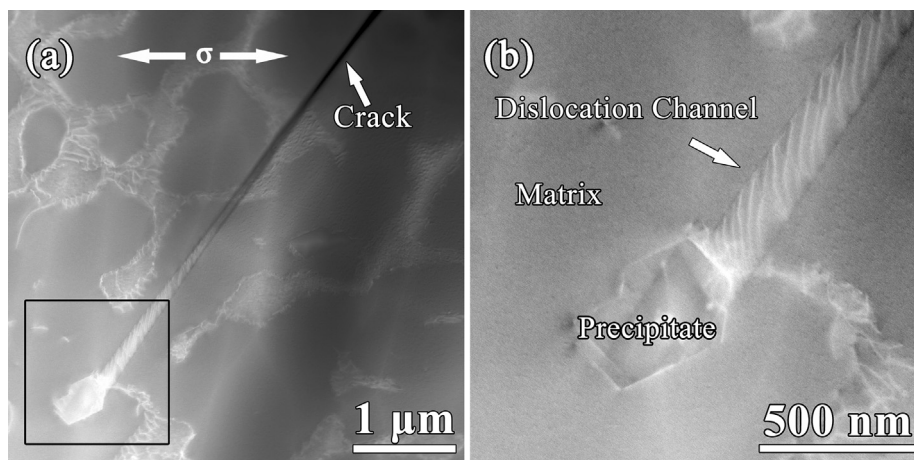


**Fig. 1.** (a) An HAADF image showing boride-containing creep microstructure, uniaxial loading direction as indicated with  $\sigma$  is parallel to  $[0\ 0\ 1]$ ; (b) a higher magnified image of the framed region in (a), displaying a dislocation channel led by a precipitate.

Download English Version:

<https://daneshyari.com/en/article/11015741>

Download Persian Version:

<https://daneshyari.com/article/11015741>

[Daneshyari.com](https://daneshyari.com)